A Small-Angle Neutron and Static Light Scattering Study of Micelles Formed in Aqueous Mixtures of a Nonionic Alkylglucoside and an Anionic Surfactant

L. Magnus Bergström*

Department of Pharmacy, Pharmaceutical Physical Chemistry, Box 580, Uppsala University, SE-751 23 Uppsala, Sweden

Luis A. Bastardo

Department of Chemistry, Surface Chemistry, Drottning Kristinas väg 51, Royal Institute of Technology, SE-100 44 Stockholm, Sweden and YKI, Institute for Surface Chemistry, Box 5607, SE-11486, Sweden

Vasil M. Garamus

GKSS Research Centre, Max Planck Street, D-215 02 Geesthacht, Germany

Received: March 4, 2005; In Final Form: April 21, 2005

The size and shape of micelles formed in aqueous mixtures of the anionic surfactant sodium dodecyl sulfate (SDS) and the nonionic sugar-based surfactant *n*-decyl β-D-glucopyranoside ($C_{10}G$) at different concentrations of added salt have been investigated with small-angle neutron and static light scattering. Rather small prolate ellipsoidal micelles form in the absence of added salt and at [NaCl] = 10 mM in D_2O. The micelles grow considerably in length to large rods as the electrolyte concentration is raised to [NaCl] = 0.1 M. In excess of nonionic surfactant ([SDS]/[$C_{10}G$] = 1:3) at [NaCl] = 0.1 M in D_2O, several thousands of Ångstroms long wormlike micelles are observed. Most interestingly, a conspicuously large isotope solvent effect was observed from static light scattering data according to which micelles formed at [SDS]/[$C_{10}G$] = 1:3 and [NaCl] = 0.1 M in H_2O are at least five times smaller than micelles formed in the corresponding samples in D_2O.

Introduction

Environmental aspects, such as the manufacture from renewable sources and biodegradability, have in recent years occasioned a rising interest in nonionic sugar-based alkyl saccharide surfactants.[1] In comparison with the more conventional nonionic polyoxyethylene surfactants, they also have a milder effect on exposure on human skin and are less sensitive to changes in temperature. In many applications a mixture of ionic and nonionic surfactants are utilized to optimize a certain desired effect. There are several reasons why surfactant mixtures behave differently from single-component surfactant systems. For instance, synergistic effects, i.e., the enhanced lowering of critical micelle concentration (cmc) and surface tension, are, as a rule, observed in mixtures of an ionic and a nonionic surfactant.[2] In addition, the size and shape of surfactant aggregates usually show a strong dependence on composition in such mixtures. Synergistic effects with respect to cmc were recently investigated for aqueous mixtures of the anionic surfactant sodium dodecyl sulfate (SDS) and the nonionic alkyl monosaccharide surfactant *n*-decyl β-D-glucopyranoside ($C_{10}G$) at different concentrations of added salt.[3] In the present paper, we investigate the size and structure of mixed SDS/$C_{10}G$ micelles formed in the absence of salt as well as at [NaCl] = 10 and 100 mM using small-angle neutron scattering (SANS) and static light scattering (SLS).

The structure of single-component alkyl saccharide micelles in D_2O have been studied with SANS in several recent works. Glucoside surfactants with a moderate chain length (C_7G, C_8G, C_9G) form micelles shaped as prolate ellipsoids or cylinders[4,5] whereas $C_{10}G$ only forms an isotropic solution of discrete micelles below surfactant concentrations of 0.l wt %. At higher concentrations, the solution phase separates as a result of the formation of very large aggregates, possibly some branched bicontinuous structure.[6] Small-angle scattering studies on octyl-β-maltoside (C_8G_2), i.e., a surfactant with a more bulky disaccharide headgroup, have shown the formation of spherical micelles that are not very sensitive to environmental conditions such as concentration and temperature,[7] whereas $C_{12}G_2$ tends to form spherical or oblate ellipsoidal micelles, depending on its stereochemical configuration (α or β).[8] $C_{14}G_2$, on the other hand, was found to form rather long and flexible ribbonlike micelles, i.e., elongated micelles with an elliptical cross section.[9] The anionic surfactant SDS forms rather small oblate ellipsoidal micelles in D_2O.[10]

Most interestingly, alkyl saccharide surfactants appear to be more sensitive to the isotopic composition of an aqueous solution, i.e., whether the solvent consists of H_2O or D_2O. Micelles formed in D_2O have been found to be slightly larger than in the corresponding samples in H_2O.[4,5,9] Moreover, a large shift in phase boundaries has been observed in the phase diagram for mixtures of C_9G and $C_{10}G$ as H_2O was substituted for D_2O.[11] It was suggested that an increased hydrophobicity of the surfactant in D_2O and/or changes in O−H/O−D bond lengths due to the exchange of hydrogen and deuterium between headgroups and solvent may cause this conspicuous isotope effect.

* Author to whom correspondence may be addressed. E-mail: magnus.bergstrom@farmaci.uu.se. Telephone: +46 18 471 43 69. Fax: +46 18 471 42 23.

10.1021/jp051113d CCC: $30.25
Published on Web 06/02/2005

Materials and Methods

Materials. Sodium dodecyl sulfate (>99%, GC) and *n*-decyl β-D-glucopyranoside (>98%, GC) were obtained from Sigma. Both surfactants were used without further purification in the neutron experiments, whereas SDS was recrystallized in ethanol at least twice prior to use in the light scattering measurements. Sodium chloride was obtained from Merck (suprapur) and used as received. Heavy water (D_2O) with 99.9 atom % D was purchased from Aldrich Chemical Co. The water used in the static light scattering experiments was obtained from a Millipore RiOs-8 and Milli-Q PLUS 185 purification system and finally filtered through a 0.2 μm Millipak filter.

Sample Preparation. Stock solutions containing sodium dodecyl sulfate (SDS) and *n*-decyl β-D-glucopyranoside ($C_{10}G$) with surfactant ratios 3:1, 1:1, and 1:3 were prepared by simply mixing the surfactants with water as well as with 10 and 100 mM aqueous solutions of NaCl to yield an overall surfactant concentration c_{surf} = [SDS] + [$C_{10}G$] = 40 mM. The final samples were then obtained by means of diluting the stock solutions to c_{surf} = 20 and 10 mM. Each sample was equilibrated for at least 15 h at 22 °C before the measurements. Heavy water (D_2O) was chosen as solvent in all neutron experiments to minimize the incoherent background from hydrogen and obtain a high scattering contrast.

Methods. Small-angle neutron scattering (SANS) experiments were carried out at the SANS-1 instrument at the Geesthach Neutron Facility GeNF, Geesthacht, Germany. A range of magnitudes of the scattering vector q from 0.005 to 0.25 Å^{-1} was covered by three or four combinations of sample-to-detector distances (0.7−9.7 m) at a neutron wavelength of 8.5 Å. The wavelength resolution was $\Delta\lambda/\lambda$ = 10% (full width at half-maximum value).

The samples were kept in quartz cells (Hellma) with a path length of 2 mm. The raw spectra were corrected for background from the solvent, sample cell, and other sources by conventional procedures.[12] The two-dimensional isotropic scattering spectra were azimuthally averaged, converted to an absolute scale, and corrected for detector efficiency by dividing by the incoherent scattering spectra of pure water measured in a 1-mm cell.[13] The scattering intensity was furthermore normalized by dividing with the concentrations in g/mL of solute (SDS and $C_{10}G$).

Throughout the data analyses, corrections were made for instrumental smearing.[14,15] For each instrumental setting, the ideal model scattering curves were smeared by the appropriate resolution function when the model scattering intensity was compared with the measured one by means of least-squares methods. The parameters in the model were optimized by means of conventional least-squares analysis, and the errors of the parameters were calculated by conventional methods.[16,17]

The average excess scattering length density per unit mass of solute for SDS in D_2O, $\Delta\rho_m = -5.14 \times 10^{10}$ cm/g, was calculated using the appropriate molecular volume, 410 Å^3, and weight, 288.38 g/mol, of the surfactant monomer. In the corresponding calculations for $C_{10}G$, it was assumed that the four hydrogen atoms sitting on each OH group on the glucose headgroup are all exchanged with deuterium atoms from the solvent D_2O molecules.[11] As a result, the partly deuterated sugar headgroup obtains a considerably lower magnitude of the scattering length density in D_2O, i.e., $\Delta\rho_m = -4.43 \times 10^{10}$ cm/g, than if no H−D exchange would have occurred. Our results, however, indicate that the scattering contrast for $C_{10}G$ is even lower (see further below). The molecular weight of $C_{10}G$ 324.2 g/mol is of course affected by the H−D exchange, whereas the corresponding molecular volume was assumed to be the same as in H_2O (471 Å^3).

Static light scattering (SLS) measurements were carried out on samples with a molar ratio [SDS]/[$C_{10}G$] = 1:3 and [NaCl] = 100 mM in D_2O as well as H_2O. The instrument at the Royal Institute of Technology consists of a BI-200SM goniometer connected to a BI-9000AT digital correlator from Brookhaven Instruments and a water-cooled Lexel 95-2 laser with maximum power of 2 W and a wavelength of 514 nm. The temperature was controlled to within ± 0.2 K. Experiments were performed at 29 different angles in the range of $15° \le \theta \le 155°$, corresponding to q values in the range of 4.26×10^{-4} Å$^{-1} \le q \le 33.2 \times 10^{-4}$ Å^{-1}. For each angle, 15 individual measurements were performed, out of which the five with the lowest intensities were picked out and subsequently averaged. The data were normalized to absolute scale intensities using toluene as a reference standard.

Data Analyses

SANS Data Analysis. The scattering cross section per unit mass of solute for a sample of monodisperse anisotropic particles can be written as follows

$$\frac{d\sigma_m(q)}{d\Omega} = \Delta\rho_m^2 M\langle F^2(q)\rangle_0\left[1 + \frac{\langle F(q)\rangle_0^2}{\langle F^2(q)\rangle_0}(S(q) - 1)\right] \quad (1)$$

where $\Delta\rho_m$ is the difference in scattering length per unit mass solute between particles and solvent and M is the molar mass of a particle.[17] The structure factor $S(q)$ is included by means of a so-called decoupling approximation,[18] valid for particles with small anisotropy.

The small micelles formed in all measured samples in the absence of added salt and in [NaCl] = 10 mM, as well as in the most dilute samples at x = 0.75 in [NaCl] = 100 mM, were best fitted with a model for ellipsoids of revolution with half-axis a and b. The orientational averaged form factor for ellipsoids is obtained by means of integrating twice over the square of the amplitude

$$F(q, r) = 3[\sin(qr) - qr\cos(qr)]/(qr)^3 \quad (2)$$

where

$$r(a,b,\phi) = \sqrt{a^2\sin^2\phi + b^2\cos^2\phi} \quad (3)$$

giving[19]

$$\langle F^2(q)\rangle_0 = \int_0^{\pi/2} F^2[q, r(a,b,\phi)]\sin\phi \mathrm{d}\phi \quad (4)$$

$\langle F(q)\rangle_0$ is obtained in an analogous way by integration over the amplitudes.

Interactions were taken into account by means of using a structure factor $S(q)$ including repulsive excluded volume interactions as well as electrostatic double-layer forces as derived by Hayter and Penfold[20] from the Ornstein−Zernike equation in the rescaled mean spherical approximation.[21]

The quality of the data (e.g., the maximum accessible scattering vector is q = 0.25 Å^{-1}) did not allow for the employment of a more detailed model where, for example, the micelles consisted of a core and a shell or were shaped as triaxial ellipsoids.

In [NaCl] = 100 mM, the micelles appear to be rather large and elongated. To reduce the computation times, we were able to write the form factor as a product of the contribution

attibutable to the length of the micelles $P_{length}(q)$ and the contribution from the particle cross section $P_{cs}(q)$, i.e.,

$$\frac{d\sigma_m}{d\Omega} = \Delta\rho_m^2 P_{length}(q) P_{cs}(q) \langle M_w \rangle \quad (5)$$

where $\langle M_w \rangle$ is the weight-average molar mass. This approximation is valid for micelles with a length much larger than the cross section dimensions.[22] The model fits could be slightly improved if an elliptical cross section with half-axes a and b were allowed for by means of writing the cross section as[23]

$$P_{cs}(q) = \frac{2}{\pi} \int_0^{\pi/2} \left[\frac{2J_1(qr(a,b,\phi))}{qr(a,b,\phi)} \right]^2 d\phi \quad (6)$$

where $r(a,b,\phi) = \sqrt{a^2 \sin^2 \phi + b^2 \cos^2 \phi}$ and $J_1(x)$ is the Bessel function of first order.

The data in all measured concentrations at $x = 0.50$ as well as in $c_{surf} = 40$ mM at $x = 0.75$ were best fitted using a scattering function for infinitely thin polydisperse rigid rods

$$P_{length} = \frac{\int N_{rod}(L) L^2 S_{rod}(q,L)\, dL}{\int N_{rod}(L) L^2\, dL} \quad (7)$$

where $N_{rod}(L)$ is the number distribution of micelles with respect to their length L and the form factor for an infinitely thin rod is given by[24]

$$S_{rod}(q,L) = \frac{2\mathrm{Si}(qL)}{qL} - \frac{4 \sin^2(qL/2)}{(qL)^2} \quad (8)$$

and

$$\mathrm{Si}(x) = \int_0^x \frac{\sin t}{t}\, dt \quad (9)$$

As the micelles grow even longer at [NaCl] = 100 mM, the corresponding scattering data could only be fitted assuming the micelles to be shaped as long flexible ribbons. Hence, we have used the following expression for the form factor

$$P_{length} = \frac{\int N_{worm}(L) L^2 S_{KP}(q, L, l_p)\, dL}{\int N_{worm}(L) L^2\, dL} \quad (10)$$

which is valid for a polydisperse collection of infinitely thin self-avoiding Kratky−Porod wormlike chains with a contour length L and persistence length l_p. The expression for the scattering function $S_{KP}(q, L, l_p)$ has been given by Pedersen and Schurtenberger.[25] We have assumed the number density of lengths for both rigid rods and wormlike micelles to follow a Schultz distribution

$$N_{\substack{rod \\ worm}}(L) = \frac{L^z}{z!} \left(\frac{z+1}{\langle L \rangle_N} \right)^{(z+1)} \exp^{-L(z+1)/\langle L \rangle_N} \quad (11)$$

where z is an exponent optimized in the fitting process and $\langle L \rangle_N$ is the number-weighted average length of the micelles. Below, we have presented our results in terms of the volume-weighted average length $\langle L \rangle = (z+2)/(z+1) \times \langle L \rangle_N$, i.e., the mean value as calculated from the probability distribution of finding an aggregated surfactant in a micelle of length L, and the corresponding relative standard deviation, $\sigma_L/\langle L \rangle = (z+2)^{-1/2}$.

In the model fits of the substantially elongated micelles at 0.1 M NaCl, interparticle interference effects were neglected because they are difficult to take into account. However, at such high electrolyte concentrations, the repulsive double-layer forces between the micelles are eliminated and excluded volume interactions are the predominant contribution to the interactions. The implications of neglecting interparticle interactions in the analysis of these data sets will be further discussed below.

SLS Data Analysis. The SLS data for samples with [SDS] + [C_{10}G] = 10, 20, and 40 mM in 0.1 M NaCl in D_2O were converted into neutron units and combined with SANS data in the model fitting analysis. However, to optimize the overlap between SLS and SANS data, we needed to scale the SANS data with about a factor of 2, indicating a lower scattering length density of C_{10}G than that estimated from calculations. Such a discrepancy in scattering length density was also confirmed when the aggregation number obtained from the fitting parameters was compared with the corresponding quantity calculated from the absolute intensity of the SANS data.

The apparent molar mass M_{app} and the root-mean-square radius of gyration R_g were determined from a partial Zimm plot as the intercept and slope, respectively, from a $cK_{SLS}/(d\sigma/d\Omega)$ versus q^2 plot on the basis of the following scattering law

$$\frac{c_{surf} K_{SLS}}{d\sigma/d\Omega} = \frac{1}{M_{app}} \left(1 + q^2 \frac{\langle R_g^2 \rangle}{3} \right) \quad (12)$$

where q is the magnitude of the scattering vector and c_{surf} is the concentration of solute (SDS and C_{10}G). The absolute scattered intensity per volume was determined from the relation

$$\frac{d\sigma}{d\Omega} = \left(\frac{d\sigma}{d\Omega} \right)_{ref} \left(\frac{n}{n_{ref}} \right)^2 \frac{I}{I_{ref}} \quad (13)$$

where I and I_{ref} are the average scattered intensities of sample and reference standard (toluene), respectively. The refractive index of an aqueous solution is $n = 1.335$ (H_2O) and $n = 1.331$ (D_2O) at the appropriate laser light wavelength $\lambda = 514$ nm, and $n_{ref} = 1.502$ for toluene. The absolute scattered intensity of toluene is $(d\sigma/d\Omega)_{ref} = 32 \cdot 10^{-6}$ cm^{-1} at $\lambda = 514$ nm. The scattering contrast constant is defined as follows

$$K_{SLS} = \frac{4\pi^2 n^2}{N_A \lambda^4} \left(\frac{dn}{dc} \right)^2 \quad (14)$$

where the refractive index increment $dn/dc = 0.126$ mL/g for [SDS]/[C_{10}G] = 1:3 in [NaCl] = 100 mM.

Results and Discussion

Small-Angle Neutron Scattering. Surfactant mixtures in D_2O with compositions $x \equiv$ [SDS]/([SDS] + [C_{10}G]) = 0.25, 0.50, and 0.75 were measured with SANS at overall concentrations $c_{surf} \equiv$ [SDS] + [C_{10}G] = 10, 20, and 40 mM in the absence of added salt, [NaCl] = 10 mM and [NaCl] = 100 mM. The results of the SANS data analyses are summarized in Table 1.

Examples of scattering data for samples in the absence of added salt as well as in [NaCl] = 10 mM are given in Figures 1 and 2, respectively. All data for these samples were best fitted with a model for ellipsoids of revolution with half-axes a and b. By optimizing a and b, it was found that prolate ellipsoids always gave a better agreement with the data than that of oblates. Comparing the results for mixed micelles with the ones corresponding to single-component micelles, it is evident that

TABLE 1: Results from the SANS and SLS Data Analyses

[NaCl] = 0	$x = 0.25$	$x = 0.50$	$x = 0.75$
40 mM	$a = 17.9$	$a = 17.4$	$a = 17.0$
	$b = 38.3$	$b = 29.2$	$b = 26.3$
	$N = 113$	$N = 85$	$N = 75$
20 mM	$a = 17.8$	$a = 17.8$	$a = 17.5$
	$b = 33.0$	$b = 27.0$	$b = 24.3$
	$N = 96$	$N = 81$	$N = 73$
10 mM	$a = 17.7$	$a = 17.7$	$a = 17.3$
	$b = 32.6$	$b = 27.6$	$b = 26.0$
	$N = 94$	$N = 82$	$N = 77$
[NaCl] = 10 mM	$x = 0.25$	$x = 0.50$	$x = 0.75$
40 mM	$a = 17.4$	$a = 18.0$	$a = 17.5$
	$b = 68.0$	$b = 32.1$	$b = 27.3$
	$N = 189$	$N = 99$	$N = 82$
20 mM	$a = 17.7$	$a = 18.0$	$a = 17.5$
	$b = 47.7$	$b = 29.2$	$b = 26.5$
	$N = 137$	$N = 90$	$N = 80$
10 mM	$a = 17.9$	$a = 17.8$	$a = 18.3$
	$b = 42.8$	$b = 30.6$	$b = 26.5$
	$N = 127$	$N = 92$	$N = 88$
[NaCl] = 100 mM	$x = 0.25$	$x = 0.50$	$x = 0.75$
40 mM	$a = 12.6$	$a = 12.6$	$a = 12.4$
	$b = 20.2$	$b = 20.3$	$b = 20.6$
	$\langle L \rangle_{app} = 1420$	$\langle L \rangle_{app} = 372$	$\langle L \rangle_{app} = 355$
	$l_p = 269$	$\sigma_L/\langle L \rangle = 0.7$	$\sigma_L/\langle L \rangle = 0.9$
	$N_{app} = 2490$	$N_{app} = 676$	$N_{app} = 671$
	$R_g = 306$ Å		
	$N_{SLS} = 2470$		
20 mM	$a = 13.5$	$a = 13.2$	$a = 18.5$
	$b = 19.2$	$b = 19.2$	$b = 33.0$
	$\langle L \rangle_{app} = 3600$	$\langle L \rangle_{app} = 502$	$N = 114$
	$l_p = 209$	$\sigma_L/\langle L \rangle = 0.95$	
	$N_{app} = 6420$	$N_{app} = 797$	
	$R_g = 453$ Å		
	$N_{SLS} = 4680$		
10 mM	$a = b = 16.5$	$a = 14.5$	$a = 18.4$
	$\langle L \rangle_{app} = 4410$	$b = 18.4$	$b = 33.0$
	$l_p = 193$	$\langle L \rangle_{app} = 326$	$N = 125$
	$N_{app} = 8230$	$\sigma_L/\langle L \rangle = 0.95$	
	$R_g = 434$ Å	$N_{app} = 621$	
	$N_{SLS} = 4940$		

the detailed structure more resembles the one for alkylglucoside micelles (elongated prolates or rods) than that of SDS micelles (oblates). From the spatial dimension obtained from the model fits, it was also possible to calculate the micelle aggregation number N from the molecular volumes of the two surfactants, assuming the composition in the micelles to equal the overall composition. Typical error bars of the fitting parameters are for $a \pm 0.5$ Å and for $b \pm 1.0$ Å.

In addition to the parameters in Table 1, the model fit was optimized with respect to effective charge and electrolyte concentration for a given surfactant concentration. These two quantities are, however, strongly intercorrelated and cannot be accurately determined from the model fitting procedure unless one of them is independently determined, for example, by measuring the free surfactant concentration in D_2O. This has not been done, and accordingly, neither of the quantities is included in Table 1.

In Figure 3, we have plotted the half axes against the composition for the different overall surfactant concentrations in the absence of salt, and Figure 4 shows the corresponding plots at [NaCl] = 10 mM. The short axis is found to be rather constant in all samples, whereas the micelles become substantially longer in the presence of salt. For both sets of samples it is clearly observed that the micelles, as expected, grow with decreasing fraction of SDS. It is also seen that the rather

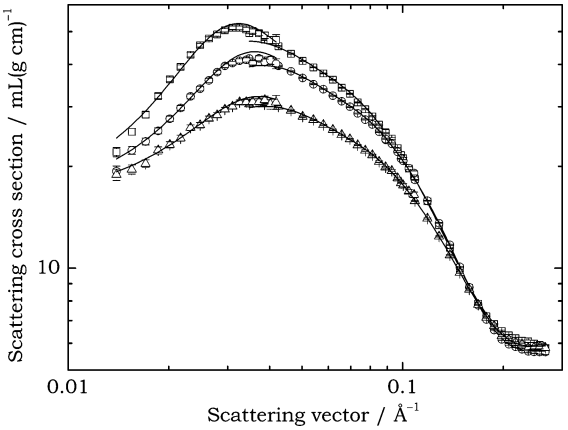

Figure 1. Normalized scattering cross section as a function of the scattering vector q for mixtures of SDS and $C_{10}G$ in the absence of added salt in D_2O. The compositions are [SDS]/[$C_{10}G$] = 1:3 (squares), [SDS]/[$C_{10}G$] = 1:1 (circles) and [SDS]/[$C_{10}G$] = 3:1 (triangles). [SDS] + [$C_{10}G$] = 20 mM for all samples. Individual symbols represent data obtained for different sample−detector distances. The solid lines represent the best available fit with a model for prolate ellipsoids of revolution with half axes a and b. The results of the fits are given in Table 1. The agreements of the fits as measured by χ^2 are 7.3 ([SDS]/[$C_{10}G$] = 1:3), 5.8 ([SDS]/[$C_{10}G$] = 1:1), and 1.4 ([SDS]/[$C_{10}G$] = 3:1).

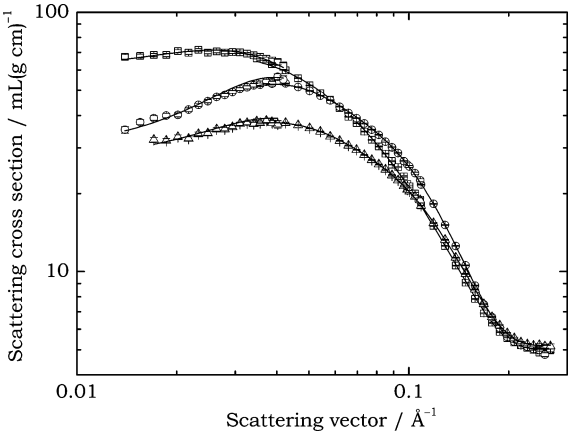

Figure 2. Normalized scattering cross section as a function of the scattering vector q for mixtures of SDS and $C_{10}G$ in [NaCl] = 10 mM in D_2O. The compositions are [SDS]/[$C_{10}G$] = 1:3 (squares), [SDS]/[$C_{10}G$] = 1:1 (circles), and [SDS]/[$C_{10}G$] = 3:1 (triangles). [SDS] + [$C_{10}G$] = 20 mM for all samples. Individual symbols represent data obtained for different sample−detector distances. The solid lines represent the best available fit with a model for prolate ellipsoids of revolution with half axes a and b. The results of the fits are given in Table 1. The agreements of the fits as measured by χ^2 are 9.0 ([SDS]/[$C_{10}G$] = 1:3), 4.0 ([SDS]/[$C_{10}G$] = 1:1), and 1.6 ([SDS]/[$C_{10}G$] = 3:1).

elongated micelles present at $x = 0.25$ grow substantially with increasing overall surfactant concentration at both electrolyte concentrations.

Examples of scattering data for samples in [NaCl] = 100 mM are given in Figure 5. By means of adding such a substantial amount of salt, the micelles become so large that the ellipsoidal model can only be employed for the two most diluted samples at $x = 0.75$. For all samples at $x = 0.50$ and the most concentrated one at $x = 0.75$ ($c_{surf} = 40$ mM), the data were best fitted with a model for polydisperse rigid rods with weight-averaged length $\langle L \rangle$ and relative standard deviation $\sigma_L/\langle L \rangle$. In this model, we have not taken into account interparticle interference effects, which means that the micelle length as obtained in the model fits is not expected to correspond to the

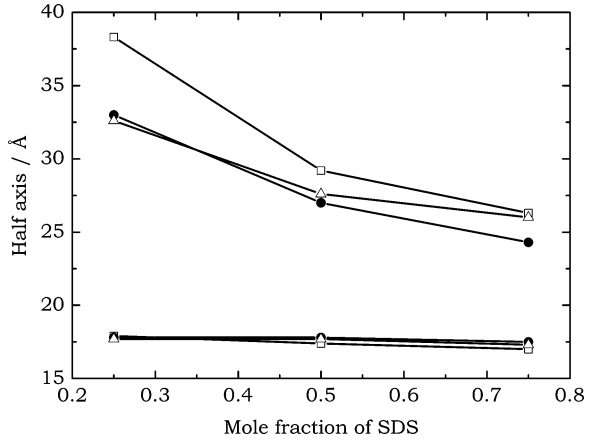

Figure 3. Half axes *a* (lower symbols) and *b* (upper symbols) of mixed SDS/C_{10}G micelles formed in the absence of added salt plotted against the mole fraction of SDS, x = [SDS]/([SDS] + [C_{10}G]). The overall surfactant concentrations are c_{surf} = 40 mM (squares), c_{surf} = 20 mM (circles), and c_{surf} = 10 mM (triangles).

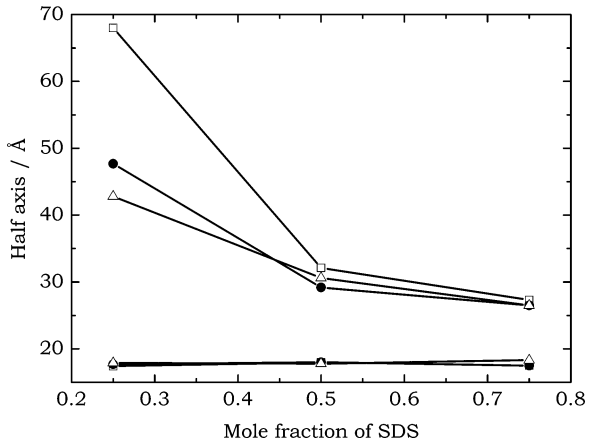

Figure 4. Half axes *a* (lower symbols) and *b* (upper symbols) of mixed SDS/C_{10}G micelles formed in [NaCl] = 10 mM plotted against the mole fraction of SDS, x = [SDS]/([SDS] + [C_{10}G]). The overall surfactant concentrations are c_{surf} = 40 mM (squares), c_{surf} = 20 mM (circles), and c_{surf} = 10 mM (triangles).

real value as the magnitude of the interactions is not negligible. Hence, the corresponding fitting parameter is an apparent micelle length denoted $\langle L\rangle_{app}$.

In the case at x = 0.50 in [NaCl] = 0.1 M, $\langle L\rangle_{app}$ is found to first increase as the overall surfactant concentration is raised from 10 to 20 mM but then decreases as c_{surf} reaches 40 mM. The composition in the micelles is expected to be approximately independent of overall surfactant concentration as c_{surf} is appreciably above the free surfactant concentration and the cmcs for the two surfactants in the absence of the other are of comparable magnitude. The cmcs for SDS and C_{10}G in 0.1 M NaCl in H_2O are 1.5 and 2.0 mM, respectively, whereas the cmc for mixed micelles equals about 1.2 mM in the range $0.2 < x < 0.8$.[3] As a result, the micelles are expected to behave as single-component micelles, i.e., to grow rapidly with increasing c_{surf}. Hence, the observed variation of $\langle L\rangle_{app}$ with surfactant concentration indicates that interactions are considerable in a magnitude above about 20 mM but vanish rapidly below this concentration.

The polydispersity $\sigma_L/\langle L\rangle$ was found to be close to unity, which is the expected value for infinitely long micelles,[26] for the less concentrated samples. The corresponding parameter in the model fit was fixed to $\sigma_L/\langle L\rangle$ = 0.95 because it is difficult to determine its exact value above about $\sigma_L/\langle L\rangle$ = 0.9. At c_{surf} = 40 mM, the polydispersity as obtained from the model fit appears to be lower, which is most likely a consequence of the omission of interparticle interactions in the data analysis.

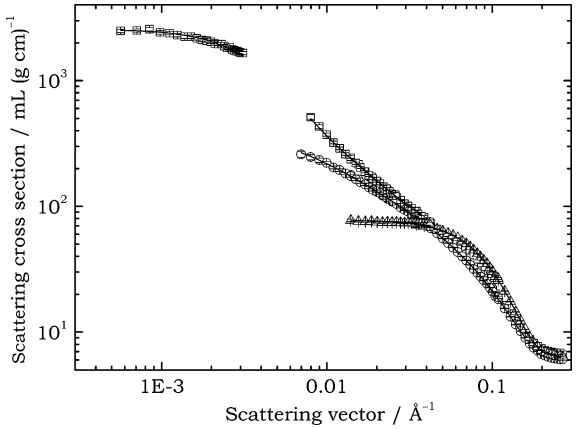

Figure 5. Normalized scattering cross section as a function of the scattering vector q for mixtures of SDS and C_{10}G in [NaCl] = 0.1 M in D_2O. The compositions are [SDS]/[C_{10}G] = 1:3 (squares), [SDS]/[C_{10}G] = 1:1 (circles), and [SDS]/[C_{10}G] = 3:1 (triangles). [SDS] + [C_{10}G] = 20 mM for all samples. Individual symbols represent SANS and SLS (squares at low q-values) data obtained for different sample−detector distances. The solid lines represent the best available fit with a model for prolate ellipsoids of revolution (triangles), polydisperse rigid rods (circles), and flexible self-avoiding wormlike micelles (squares). The results of the fits are given in Table 1. The agreements of the fits as measured by χ^2 are 1.5 ([SDS]/[C_{10}G] = 1:3), 1.0 ([SDS]/[C_{10}G] = 1:1), and 1.3 ([SDS]/[C_{10}G] = 3:1).

At x = 0.25 in [NaCl] = 100 mM, the micelles have further grown and were best fitted with a model for flexible wormlike micelles with an apparent contour length $\langle L\rangle_{app}$ and persistence length l_p. The micelles are seen to be considerably larger than at x = 0.50, i.e., several thousands of Ångstroms. Hence, we have also included static light scattering data in the analysis, which gives relevant information in the low q regime [cf. Figure 5]. Because there is a slight gap between the SLS and SANS data sets, it was not possible to determine the polydispersity for these samples. Here, $\langle L\rangle_{app}$ is seen to decrease with surfactant concentration in the entire regime that was measured, indicating that interactions between the very large micelles influence the scattering data also in the regime of lowest measured concentrations. Because the length of rod-shaped and wormlike micelles is expected to rapidly increase in magnitude with surfactant concentration, we expect $\langle L\rangle$ at 20 and 40 mM to be considerably larger than its determined value at 10 mM ($\langle L\rangle_{app}$ = 4410 Å).

The persistence length as obtained from the model fits is also expected to be influenced by interactions between the micelles, and it is seen to decrease with decreasing surfactant concentration. An extrapolation to zero concentration gives a value of l_p = 163 Å for the persistence length at x = 0.25 and [NaCl] = 0.1 M. This is slightly less than 178 Å, which was obtained for pure wormlike SDS micelles in 1.0 M NaBr.[10] A lower value of l_p for the mixed micelles is expected because the hydrocarbon chain length of C_{10}G is slightly shorter than that of SDS.

The agreement between data and models for rigid or flexible elongated micelles could be slightly improved if an elliptical cross section with half-axis *a* and *b* of the micelles were allowed for. The axial ratio is found to be about 1.6 for the samples at c_{surf} = 40 mM and decreases with decreasing surfactant concentration. However, the model fit could also be improved to an equally large extent by means of employing a core and shell model with scattering length densities as calculated from the detailed molecular structure of the surfactants. In this case,

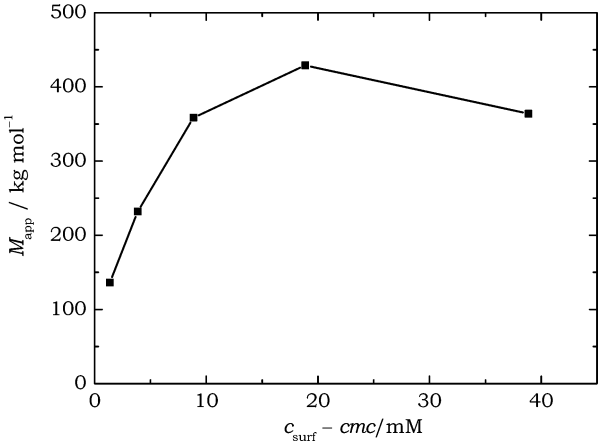

Figure 6. Apparent molar mass M_{app} of mixed SDS/C_{10}G micelles at [SDS]/[C_{10}G] = 1:3 and [NaCl] = 0.1 M in H_2O as obtained from partial Zimm plots of SLS data plotted against surfactant concentration. The latter quantity was obtained by subtracting the free surfactant concentration at cmc from the overall surfactant concentration.

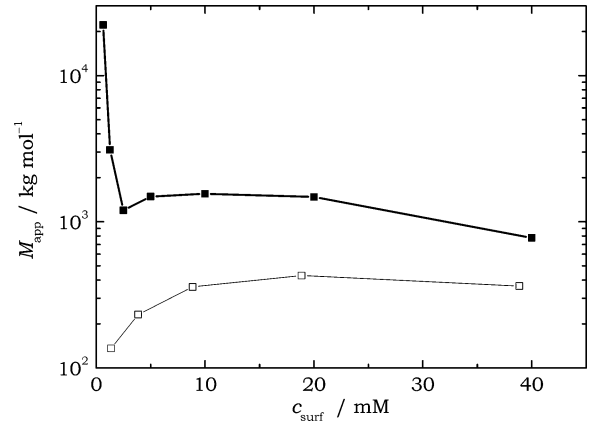

Figure 7. Apparent molar mass M_{app} of mixed SDS/C_{10}G micelles at [SDS]/[C_{10}G] = 1:3 and [NaCl] = 0.1 M in D_2O as obtained from partial Zimm plots of SLS data plotted against overall surfactant concentration (solid squares). We have also included the corresponding M_{app} in H_2O as a function of $c_{surf} - cmc$ (open squares, same plot as in Figure 6).

the thickness of the inner core varies between 13.6 and 15.6 Å and the outer core between 0 and 11.8 Å. Because data above $q = 0.25$ Å^{-1} are missing, we are not able to distinguish between the two models.

Static Light Scattering. Samples with $x = 0.25$ and 100 mM NaCl, in D_2O as well as in H_2O, were investigated by static light scattering. From partial Zimm plots, an apparent molar mass M_{app} and radius of gyration R_g of the micelles was determined. An apparent aggregation number N_{SLS} was obtained by simply dividing M_{app} with the appropriate surfactant molar mass and is included in Table 1 together with R_g. M_{app} is plotted against surfactant concentration in H_2O and D_2O in Figures 6 and 7, respectively. In the former case, the free surfactant concentration at cmc, as determined by surface tension measurements[3], was subtracted from c_{surf}. The apparent molar mass is related to the weight-average molecular weight as $M_{app} = S(0)^*\langle M_w\rangle$ where $S(0)$ is the structure factor at $q = 0$. $S(0) < 1$ as a result of repulsive interactions between the micelles and approaches unity as the overall concentration vanishes. As a consequence, M_{app} is seen to decrease with increasing surfactant concentration at high values of c_{surf}. As c_{surf} decreases, M_{app} approaches $\langle M_w\rangle$, and we observe the typical increase in micelle size with increasing surfactant concentration at low values of c_{surf}.

Most interestingly, an enormous solvent isotope effect is evident from the results shown in Figures 6 and 7. M_{app} is considerably larger in D_2O (about a factor 5 or so) than in H_2O. Considering the fact that structure factor effects are more significant for the substantially larger micelles in D_2O, the difference in micelle size is expected to be even more pronounced than what appears in Figure 7. Moreover, the micelle size appears to rapidly increase with decreasing surfactant concentration below $c_{surf} = 2.5$ mM in D_2O. As a matter of fact, very large aggregates are still present at $c_{surf} = 0.625$ mM, i.e., well below the critical micelle concentration for the same composition in H_2O ($cmc = 1.2$ mM)[3], clearly demonstrating that cmc also is lowered when the solvent is switched to heavy water. An unusually large solvent isotope effect on the size of micelles formed by sugar-based surfactants has been previously reported[4,5] but not as conspicuous as the one observed here.

A dramatic shift of the phase boundaries in a phase diagram for mixtures of C_9G or C_{10}G, as H_2O was substituted for D_2O, was recently observed by Whiddon and Söderman.[11] It was suggested that the effect was due to an increased hydrophobicity of the surfactant in D_2O or as a result of reduced steric headgroup repulsions caused by a shift in O−H and O−D bond lengths as hydrogen atoms are exchanged with deuterium atoms from the solvent molecules. Both of these effects may also rationalize an increased size of elongated micelles in D_2O. The reason is that elongated micelles are stabilized in a different manner as compared to that of spherical or disklike micelles.[26−28] As a result, the former are expected to be very polydisperse as well as to grow considerably with increasing surfactant concentration. As a consequence, small changes in environmental conditions may imply dramatic changes in micelle size in regions where the micelles are considerably elongated. This kind of behavior has been observed, for instance, as the temperature is varied in ionic surfactant systems.[29]

In the present case, the increased micelle size was linked to a considerable decrease in cmc, indicating an increased hydrophobicity of C_{10}G in D_2O as compared with that of H_2O. The sharp increase in aggregate size upon decreasing the overall surfactant concentration at low values of c_{surf} [cf. Figure 7] may then be explained as the result of an increasing fraction of the nonionic surfactant aggregated in the micelles as c_{surf} is reduced below the free concentration of the ionic surfactant. A similar effect has previously been observed in mixtures of an anionic and a cationic surfactant.[23,30,31]

Conclusions

The size and geometrical shape of micelles formed in mixtures of SDS and the nonionic alkylglucoside C_{10}G in D_2O have been investigated with small-angle neutron scattering. The observed micelles were generally found to be elongated. Prolate ellipsoidal micelles form at low electrolyte concentrations ([NaCl] = 0 and 10 mM), which grow substantially in length when [NaCl] is raised to 100 mM. In the latter case, rigid rods appeared at surfactant compositions [SDS]/[C_{10}G] = 3:1 and 1:1, whereas very long flexible wormlike micelles were observed in excess of alkylglucoside, i.e., at [SDS]/[C_{10}G] = 1:3. The size of the wormlike mixed micelles in the latter samples was further investigated with static light scattering. Most interestingly, the size of elongated micelles formed at [SDS]/[C_{10}G] = 1:3, and [NaCl] = 100 mM was found to be at least five

times larger in heavy water (D_2O) than in conventional water (H_2O). To the authors' knowledge, such a large solvent isotope effect on the size of surfactant micelles has previously never been reported. The corresponding critical micelle concentration was also reduced by at least a factor of 2, indicating an increased hydrophobicity of the alkylglucoside surfactant in D_2O. Nevertheless, this unusually large impact of heavy water on the behavior of sugar-based surfactants needs to be further investigated to be fully understood.

Acknowledgment. This work was supported by the Swedish Competence Center for Surfactants Based on Natural Products (SNAP).

References and Notes

(1) Söderman, O.; Johansson, I. *Curr. Opin. Colloid Interface Sci.* **2000**, *4*, 391.
(2) Holland, P. M.; Rubingh, D. N. *J. Phys. Chem.* **1983**, *87*, 1984.
(3) Bergström, M.; Jonsson, P.; Persson, M.; Eriksson, J. C. *Langmuir* **2003**, *19*, 10719.
(4) Zhang, R.; Marone, P. A.; Thiyagarajan, P.; Tiede, D. *Langmuir* **1999**, *15*, 7510.
(5) Ericsson, C.; Söderman, O.; Garamus, V. M.; Bergström, M.; Ulvenlund, S. *Langmuir* **2004**, *20*, 1401.
(6) Nilsson, F.; Söderman, O.; Hansson, P.; Johansson, I. *Langmuir* **1998**, *14*, 4050.
(7) He, L.-Z.; Garamus, V. M.; Funari, S. S.; Malfois, M.; Willumeit, R.; Niemeyer, B. *J. Phys. Chem. B* **2002**, *106*, 7596.
(8) Dupuy, C.; Auvray, X.; Petipas, C.; Rico-Lattes, I.; Lattes, A. *Langmuir* **1997**, *13*, 3965.
(9) Ericsson, C. A.; Söderman, O.; Garamus, V. M.; Bergström, M.; Ulvenlund, S. *Langmuir* **2005**, *21*, 1507.
(10) Bergström, M.; Pedersen, J. S. *Phys. Chem. Chem. Phys* **1999**, *1*, 4437.
(11) Whiddon, C.; Söderman, O. *Langmuir* **2001**, *17*, 1803.
(12) Cotton, J. P. *Neutron, X-ray and Light Scattering: Introduction to an Investigative Tool For Colloidal and Polymeric Systems;* Lindner, P., Zemb, T., Eds.; North-Holland: Amsterdam, 1991.
(13) Wignall, G. D.; Bates, F. S. *J. Appl. Crystallogr.* **1986**, *20*, 28.
(14) Pedersen, J. S. *J. Phys. IV* **1993**, *3*, 491.
(15) Pedersen, J. S.; Posselt, D.; Mortensen, K. *J. Appl. Crystallogr.* **1990**, *23*, 321.
(16) Bevington, B. R. *Data Reduction and Error Analysis for Physical Sciences*; McGraw-Hill: New York, 1969.
(17) Pedersen, J. S. *Adv. Colloid Interface Sci.* **1997**, *70*, 171.
(18) Kotlarchyk, M.; Chen, S. H. *J. Chem. Phys.* **1983**, *79*, 2461.
(19) Mittelbach, P.; Porod, G. *Acta Phys. Austriaca* **1962**, *15*, 122.
(20) Hayter, J. B.; Penfold, J. *Mol. Phys.* **1981**, *42*, 409.
(21) Hansen, J. P.; Hayter, J. B. *Mol. Phys.* **1982**, *46*, 651.
(22) Pedersen, J. S.; Schurtenberger, P. *J. Appl. Crystallogr.* **1996**, *29*, 646.
(23) Bergström, M.; Pedersen, J. S. *J. Phys. Chem. B* **1999**, *103*, 8502.
(24) Neugebauer, T. *Ann. Phys. (Leipzig)* **1943**, *42*, 509.
(25) Pedersen, J. S.; Schurtenberger, P. *Macromolecules* **1996**, *29*, 7602.
(26) Bergström, M. Thermodynamics of Micelles and Vesicles. In *Handbook of Surfaces and Interfaces of Materials*; Nalwa, H. S., Ed.; Academic Press: San Diego, 2001; Vol. 5, p 233.
(27) Eriksson, J. C.; Ljunggren, S.; Henriksson, U. *J. Chem. Soc., Faraday Trans. 2* **1985**, *81*, 833.
(28) Eriksson, J. C.; Ljunggren, S. *J. Chem. Soc., Faraday Trans. 2* **1985**, *81*, 1209.
(29) Mazer, N. A.; Benedek, G. B.; Carey, M. C. *J. Phys. Chem.* **1976**, *80*, 1075.
(30) Bergström, M.; Pedersen, J. S. *Langmuir* **1999**, *15*, 2250.
(31) Bergström, M.; Pedersen, J. S.; Schurtenberger, P.; Egelhaaf, S. U. *J. Phys. Chem. B* **1999**, *103*, 9888.